Journal of Applied Electrochemistry (2006) 36:33–41
DOI 10.1007/s10800-005-9011-0

Impedance spectroscopy study of anodic growth of thick zirconium oxide films in H_2SO_4, Na_2SO_4 and NaOH solutions

THIERRY PAUPORTÉ* and JÖRGEN FINNE
Laboratoire d' Electrochimie et Chimie Analytique, Ecole Nationale Supérieure de Chimie, UMR 7575, 11 rue P. et M. Curie, 75231, Paris cedex 05, France
*(*author for correspondence, e-mail: thierry-pauporte@enscp.fr.)*

Received 8 December 2004; accepted in revised form 26 May 2005

Key words: anodic oxidation, impedance spectroscopy, zirconium

Abstract

Anodic zirconium oxide films were grown potentiodynamically at a constant sweep rate up to the breakdown potential on rod electrodes made of 99.8% metallic zirconium. Different media of different pH were tested, namely 0.5 M H_2SO_4 (pH 0.3), 0.1 M Na_2SO_4 (pH 9) and 0.1 M NaOH (pH 13). By electrochemical impedance spectroscopy and scanning electron microscopy the oxide film thickness was monitored during the voltage scan. The behaviour was found to be different in the presence and absence of sulphate anions. In the presence of SO_4^{2-}, the films were dense but breakdown occurred at 300–340 nm. In NaOH, two relaxations appeared above 50 V and were ascribed to a bi-layered coating structure and the maximum layer thickness was 720 nm before breakdown.

1. Introduction

ZrO_2 is an insulator with a large bandgap at 5 eV [1]. This oxide has potential applications in various fields such as protective coatings [2], dielectric compounds in metal oxide semiconductor devices and as a high temperature O^{2-} conducting electrolyte, important in sensors and fuel cell applications [3]. Thick oxide films can be obtained by sputtering, pulsed laser deposition, chemical vapor deposition and atomic layer epitaxy [3] and also by wet methods such as anodisation. This latter technique is based on the anodic electrochemical oxidation of the metal [4, 5]. In the case of dielectric oxide films formed by anodisation, a high electric field must be maintained in the layer in order to control the growth kinetics. It is well-documented that in the case of zirconia the growth rate is almost exclusively limited by O^{2-} migration from the film/electrolyte interface towards the metal/oxide interface. O^{2-} is produced by water dissociation. Metallic zirconium is oxidized in Zr^{4+} at the metal/oxide interface where it reacts with O^{2-} supplied by migration. The transport number of Zr^{4+} is almost zero [4, 5]. The film growth reactions are thus:

$$Zr \Rightarrow Zr^{4+} + 4e^- \quad (1a)$$

$$Zr^{4+} + 2O^{2-} \Rightarrow ZrO_2 \quad (1b)$$

Although the anodisation of metallic zirconium has been widely studied, many workers have focused their attention on the low voltages (below 10 V) (e.g. [1, 6–8]). The voltage limit that can be reached prior to film breakdown has been described as increasing with electrolyte resistivity and current density [9]. It also depends upon the anion [9]. However, whatever the growth condition used, the breakdown voltage limit given in the literature never exceeds 300 V [10]. A maximum film thickness of 400 nm has been reported for films grown at 24 mA cm^{-2} in 0.05 N H_2SO_4 [10]. Leach and Pearson [11] studied the formation of anodic ZrO_2 at 200 V in ammonium borate (pH 9) at 0.01 mA cm^{-2} before disruption and blistering occurred. Wood and Pearson [12] reported oxide films grown galvanostatically on Zr in an ammonium tartrate solution. The breakdown (sparking) occured at 300 V and anodisation could be continued up to 440 V in spite of this phenomenon. The film was described as non-homogeneous, consisting of trails of crystalline zirconia and patches of white powder.

The present work aims at investigating the influence of the electrolytic solution (anion, pH) on the growth of thick anodic oxide films at high voltage and up to the breakdown potential. The film electrical properties, the growth constant (defined as the relationship between the film thickness and the applied voltage) and the microstructure of the films, have been studied with help

of a non-destructive procedure based on electrochemical impedance spectroscopy (EIS).

2. Experimental details

2.1. *Electrode preparation*

The electrodes were made of zirconium rods of purity 99.8% (Goodfellow), 1.5 mm in diameter and 5–10 mm in length. The main impurity contents were 2500 ppm Hf, 250 ppm C, 200 ppm Cr and 200 ppm Fe. They were sealed in a glass tube with an epoxy resin. In a preliminary study, several sealing modes were tested and it was shown that this epoxy sealing gives the best results in terms of highest voltage attained before breakdown. After a first mechanical polishing with P400 and P1200 abrasive papers, the electrodes were finally polished with a 3 μm diamond powder on a metallurgical cloth. They were subsequently degreased for 5 min in acetone and then for 5 min in ethanol in an ultrasonic bath and then chemically etched for 2 min in a solution of (1:15:34) volume mixture of reagent grade 48% HF: 68% HNO_3: deionized water (18.2 MΩ cm). After the etching, the initial electrode surface state was checked by recording a first impedance spectrum at -1 V vs MSE (mercurous sulphate electrode, with a potential of $+0.65$ V vs NHE, for a normal hydrogen electrode), a potential close to the rest potential. The surface capacitance of the etched electrode was determined from this spectrum. An electrode was etched only once and each new anodisation experiment was performed with a new rod.

2.2. *Anodisation process and impedance measurements*

The aqueous electrolytic solutions were (i) 0.5 M H_2SO_4 from ultrapure 96% H_2SO_4 (Normatom from Prolabo) (pH 0.3), (ii) 0.1 M Na_2SO_4 (Aldrich, reagent grade) with a pH adjusted at 9 by NaOH addition and (iii) 0.1 M NaOH (Prolabo, reagent grade) (pH 13). The anodisation was performed in a two electrode configuration, the counter electrode being a cylindrical titanium grid covered by an IrO_2 coating. The Zr rod electrode was placed in the center of the cylinder. The applied potential during anodisation will be referred to the IrO_2 electrode. During the voltage sweeps, the solution was stirred vigorously with a magnetic barrel. The potential sweep was started at 0 V vs IrO_2 and performed at a constant sweep rate, noted v_b (classically 100 mV s^{-1} or 25 mV s^{-1}) with a Keithley 2410 sourcemeter. The voltage sweep was stopped at a given potential, E_{stop}, and an impedance spectrum was recorded then at 0 V vs MSE, a potential close to the electrode rest potential. The voltage sweep was then continued from E_{stop} to a new higher potential and stopped again for an impedance measurement at 0 V and so on. The AC measurements were done with an EG&G PAR 283 potentiostat combined with a Solartron 1255 model frequency response analyser both monitored by the Zplot-2 software from Scribner Associate. The frequency range was 1 or 10 Hz to 200 kHz with 10 points per decade. The AC amplitude was 30 mV. The spectra were fitted and analysed with help of the Zview-2 software package.

2.3. *Direct SEM observation of oxide coating*

The oxidized rods were embedded in an epoxy resin (EPOFIX from Struers) in an aluminium cylindrical sample holder and the cross-section was carefully polished with abrasive P1200 paper and on metallurgical cloths with diamond pastes of decreasing size: 6, 3, 1, 0.25 and 0.1 μm. The samples were cleaned with ethanol after each step. The cross section was then observed by scanning electron microscopy, SEM (Stereoscan 440 from Leica) in the backscattering mode.

3. Results

Figure 1a shows the variation of the current density in the sulphate media during a voltage scan at 100 mV s^{-1}.

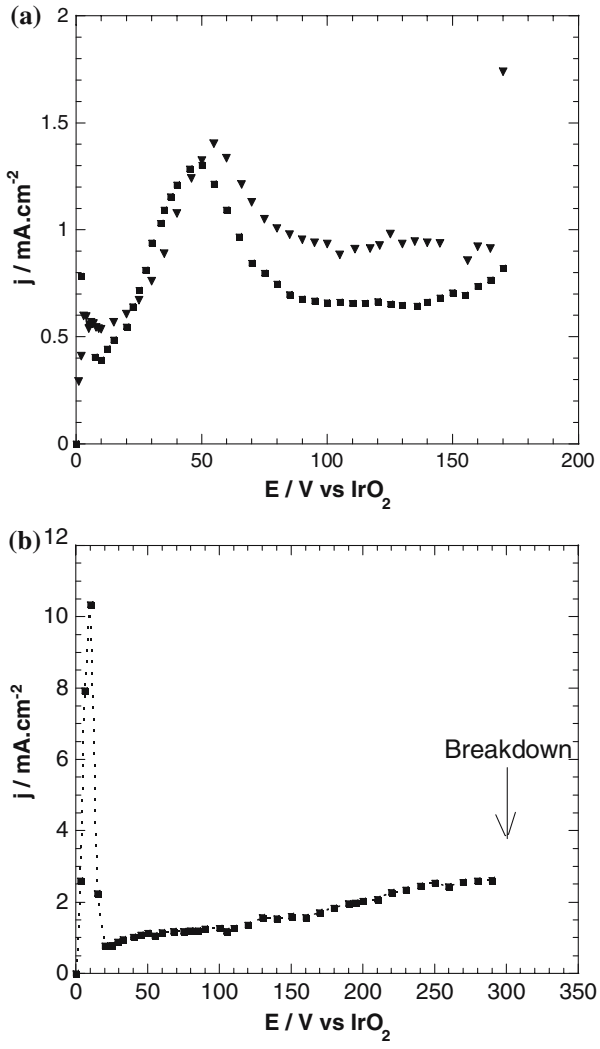

Fig. 1. Variation of current density during the potentiodynamic anodisation of metallic zirconium at 100 mV s^{-1}: (a) in 0.5 M H_2SO_4 (■) and 0.1 M Na_2SO_4 (▼); (b) in 0.1 M NaOH.

The global shape is complex but is strikingly similar at pH 0.3 and 9. After a small peak at low voltage, most likely due to oxygen evolution before electrode passivation, there is a large current peak between 20 and 80 V. Between 80 and 170 V the current density remains almost constant and forms a plateau. The current density increases with solution pH. At 100 mV s^{-1} breakdown was observed at circa 180 V in H_2SO_4 and 190–205 V in the Na_2SO_4 medium. In both cases breakdown is not due to a film homogeneous failure but to intense corrosion localised near the seal. The electrolyte is brought in contact with the bare metal, a violent current leakage is produced and a flame is observed in the vicinity of the epoxy seal.

The current density behaviour is rather different in NaOH (Figure 1b). A large current peak is observed at low voltage (0–15 V) which can be ascribed to the oxygen evolution reaction occurring before passivation of the surface. Afterwards, the current density is not constant but slowly increases with applied voltage. Its maximum at 100 mV s^{-1} before breakdown is 2.5 mA cm^{-2}. The breakdown mechanism is similar to that observed in sulphate media but occurs at a significantly higher voltage (circa 300 V).

The fact that a zirconium oxide surface layer is grown during the anodic scan can be observed directly by scanning electron microscopy (SEM). Cross-sections of samples anodised in different media are displayed in Figure 2. They were observed in the backscattering mode and the anodic oxide appears dark compared to the metal. The film thickness can be determined directly from these observations and the layer thickness growth with the increasing applied voltage is clearly observed.

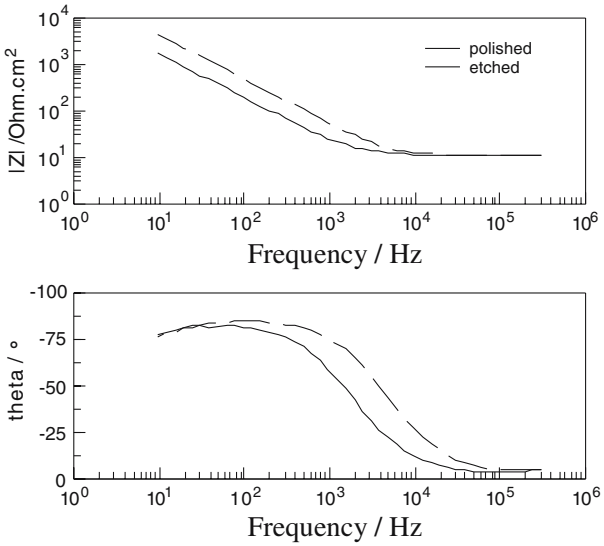

Fig. 3. Effect of HF electrode surface etching on impedance spectra in a Bode representation (measured in 0.1 M NaOH at −1 V vs MSE). Full line: polished electrode; dashed line: etched electrode.

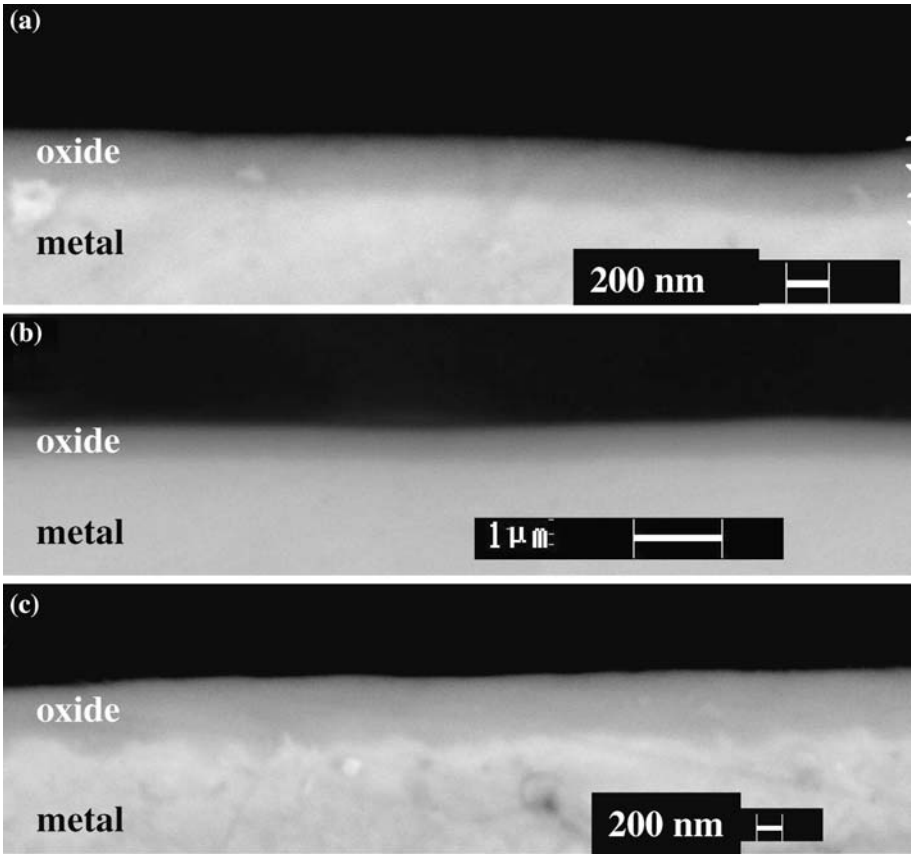

Fig. 2. SEM views of sample cross-sections. (a) film grown at 150 V in H_2SO_4 ($v_b = 25$ mV s^{-1}, $d = 250$ nm), (b) film grown at 190 V in Na_2SO_4 ($v_b = 100$ mV s^{-1}, $d = 320$ nm) and (c) film grown at 225 V in 0.1 M NaOH ($v_b = 100$ mV s^{-1}, $d = 500$ nm).

Electrochemical impedance spectroscopy was used to follow the variations of the electrode electrical behaviour with etching treatment (Figure 3) and increasing applied voltage (Figure 4a–c). The main effect of electrode etching is an increase in the impedance modulus, $|Z|$, below 10 kHz. A high frequency resistance, mainly due to the electrolytic solution, remains constant (Figure 3). The impedance response of the electrodes upon anodisation in sulphate media and in sodium hydroxide can be distinguished (Figure 4). In the first

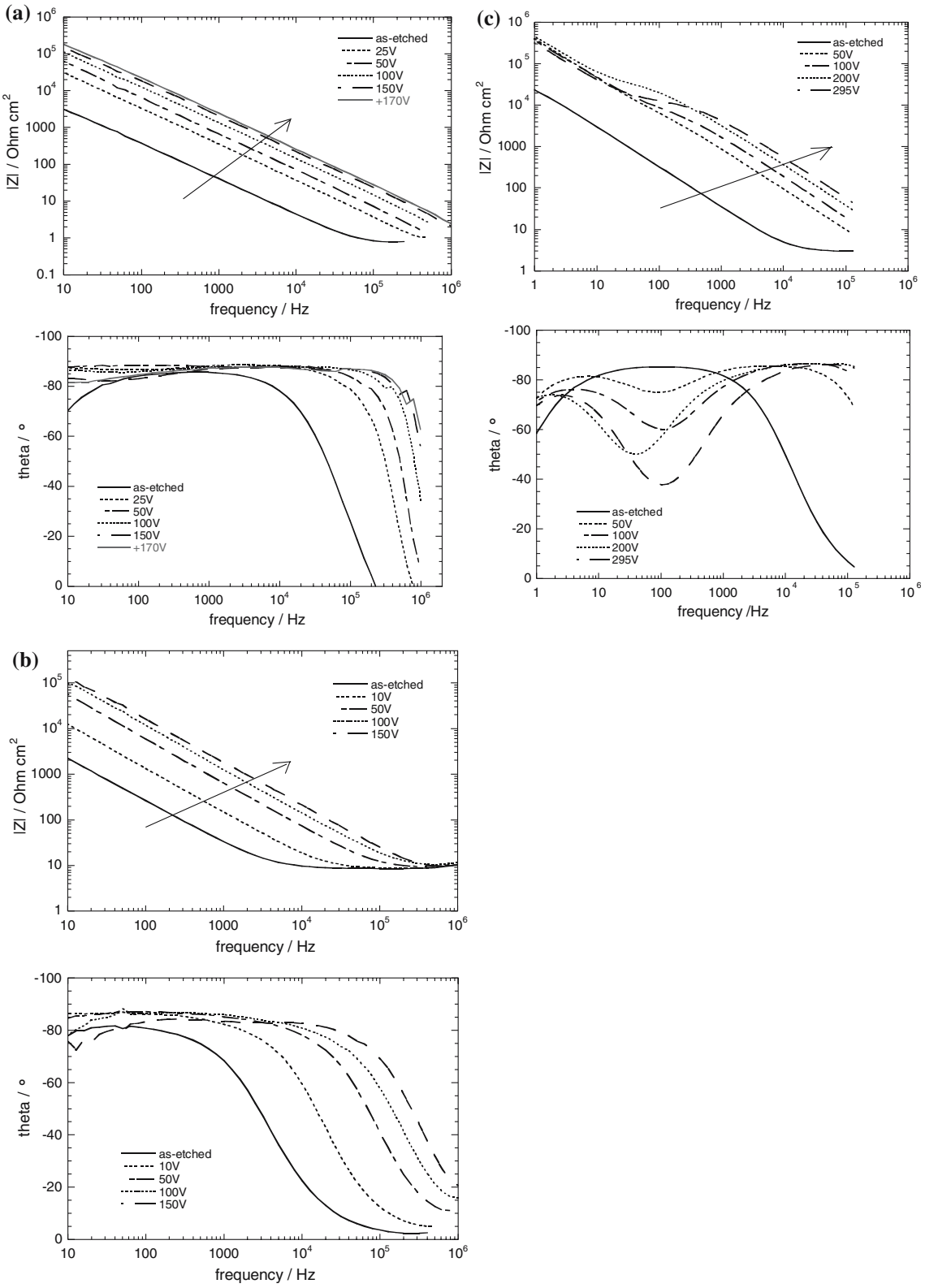

Fig. 4. Effect of the applied voltage on the electrode impedance. (a) 0.5 M H_2SO_4, (b) 0.5 M Na_2SO_4 and (c) 0.1 M NaOH. (The arrows point out the effect of increasing voltage. The etched samples spectra are measured at −1 V vs MSE).

case a single relaxation is observed (Figure 4a, b). The impedance modulus increases continuously with applied voltage over almost all the frequency range investigated. In NaOH, two relaxations appear rapidly as clearly observable on the phase part of the bode diagrams (Figure 4c). The global behaviour of the high frequency relaxation is close to that reported in sulphate media, with an increase in impedance modulus with applied voltage. In contrast, the modulus of the low frequency relaxation varies weakly with increasing applied voltage. The transition between the two regions is located at approximately 100 Hz. From the various SEM observations, it seems reasonable to ascribe the increase in the impedance modulus to the growth of the insulating anodic zirconia layer.

4. Discussion

4.1. *Equivalent circuit of the impedance spectra*

Figure 5a, c shows the two different equivalent circuits used to fit the different spectra reported in the previous section. The simplest one (Figure 5a) presents a resistance in series with a constant phase element, noted CPE, whose impedance varies according to $Z_{\mathrm{CPE1}} = \frac{1}{A_1(jw)^n}$ with $0.5 < n < 1$. Therefore, the imaginary part of the impedance spectra is not purely capacitive but affected by some dispersion (slope of the modulus is higher than -1). This equivalent circuit was used to describe the full impedance spectra of polished and as-etched electrodes, of electrodes anodised in H_2SO_4 and Na_2SO_4 up to the breakdown voltage and in NaOH up to 25 V. The high frequency part (above 1 kHz) of the spectra of electrodes anodised in NaOH at higher voltage was also fitted with this equivalent circuit. We can ascribe the CPE element to the electrical response of the surface layer and the resistance R_1 to the electrolytic solution resistance and to the contacts (Figure 5a). R_1 can be easily determined from the high frequency limit of the real part of the impedance measured at -1 V vs MSE of the as-etched samples before starting the anodisation experiment.

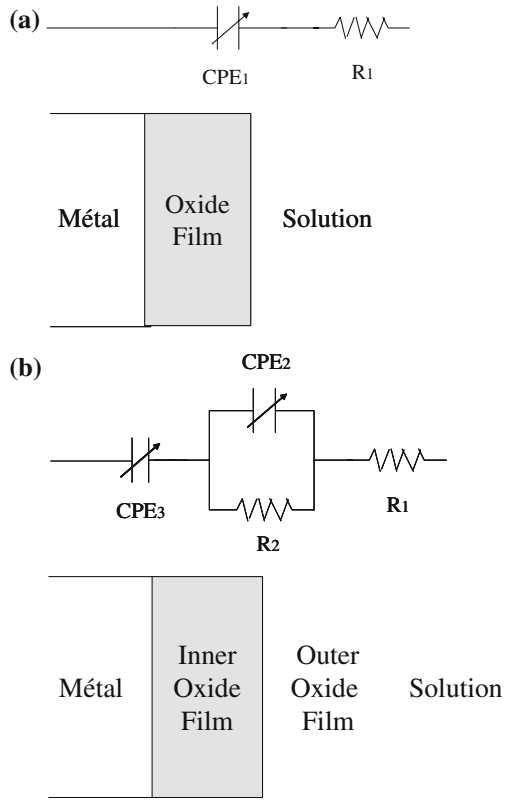

Fig. 5. Equivalent circuit used for the analysis of the EIS spectra. (a) circuit for the determination of the total oxide layer thickness. (b) Equivalent circuit used to fit the full spectra in NaOH above 25 V.

In NaOH, above 25 V the full electrical response is more complex with two different relaxations. The equivalent circuit is displayed in Figure 5b. Figure 6 shows that the experimental spectra are well-fitted with this equivalent circuit. The meaning of the low frequency relaxation is discussed in Section 4.6.

Some authors [2, 13, 14] have proposed that the dispersion is due to a dielectric constant variation with frequency in the case of ZrO_2 films obtained by corrosion at high pressure and high temperature of metallic zirconium [2] and zirconium alloys [2, 13, 14]. The film capacitance is then written as a complex term, noted C^*, for which Jonsher [15–17] has proposed the following variation with the angular frequency, ω:

$$C^* = C_\infty + \frac{B}{(j\omega)^{1-m}} \tag{2}$$

C_∞ is a pure capacitance related to the oxide thickness, B is a constant related to the dielectric dispersion and m a constant parameter. Figure 7 shows the spectra of films grown in different media in a Cole–Cole representation after the subtraction of the high frequency resistance, R_1. We do not obtain a straight line crossing the abscissa as expected from Equation (2). Accordingly, this impedance analysis procedure seems not to be suitable in the present case. The electrical behaviour of films grown by anodisation at room temperature and atmospheric pressure and those obtained by corrosion at high pressure and high temperature seems rather different.

4.2. *Determination of film capacitance and thickness*

The dispersion is likely due to some inhomogeneities in the film. The problem in the present case is to extract the film capacitance, C_f, and to get rid of the dispersion phenomena. For this purpose, we have used the general approach proposed by Brug et al. [18] in the case of a capacitance affected by some distribution of the relaxation frequency. In the present study we have supposed that the dielectric layer is not the double layer as in [18] but the oxide film. We can write:

$$C_f = \left[A_1 \left(\frac{1}{R_1} \right)^{n-1} \right]^{1/n} \tag{3}$$

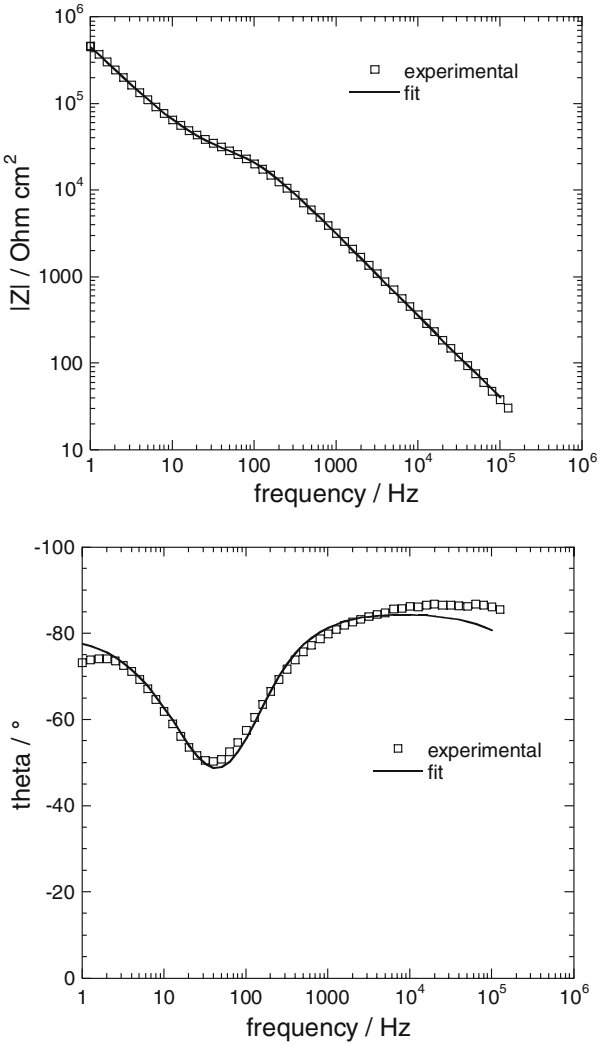

Element	R_1 /Ω	R_2/Ω	A_2/ F.Hz^{1-n2}	n_2	A_1/ F.Hz^{1-n1}	n_1
Value	5.22	36343	5.02 10^{-8}	0.977	2.48 10^{-7}	0.891
Error/ %		3.6	4.6	0.67	2.3	0.79

Fig. 6. Experimental spectrum, fitted curve and fitting parameters of the impedance response of a sample anodised in NaOH at 200 V.

The measured capacitance is in fact the contribution of two capacitances in series, namely the oxide film capacitance, C_f, and the double layer capacitance, C_{dl}, which usually exceeds 20 μF cm^{-2} at oxide electrodes in concentrated electrolyte [19]. In the present case we have found starting values classically ranging between 3–5 μF cm^{-2}. This shows that after chemical etching, a thin oxide layer is present which will be further analysed in Section 4.2. The double layer capacitance is high compared to the capacitance of the pre-existing or grown surface oxide film and has been neglected.

From C_f, determined by Equation (3), the film thickness, d, is calculated by the relationship:

$$d = \frac{\varepsilon\varepsilon_0 S}{C_f} \quad (4)$$

where ε_0 is the permittivity of vacuum (8.85×10^{-14} F cm^{-1}), ε the dielectric constant of the oxide and S the real surface area, which includes the roughness factor. We will assume in the following that the roughness factor is 1. As shown below, ε is found to be close to 20 and relatively independent on the growth medium.

4.3. *Surface state of the as-prepared electrode after etching in HF*

After chemical etching, the zirconium surface becomes bright and mirror like. Figure 3 compares the impedance spectra recorded after a simple polishing of the surface with a 3 μm diamond paste and after a

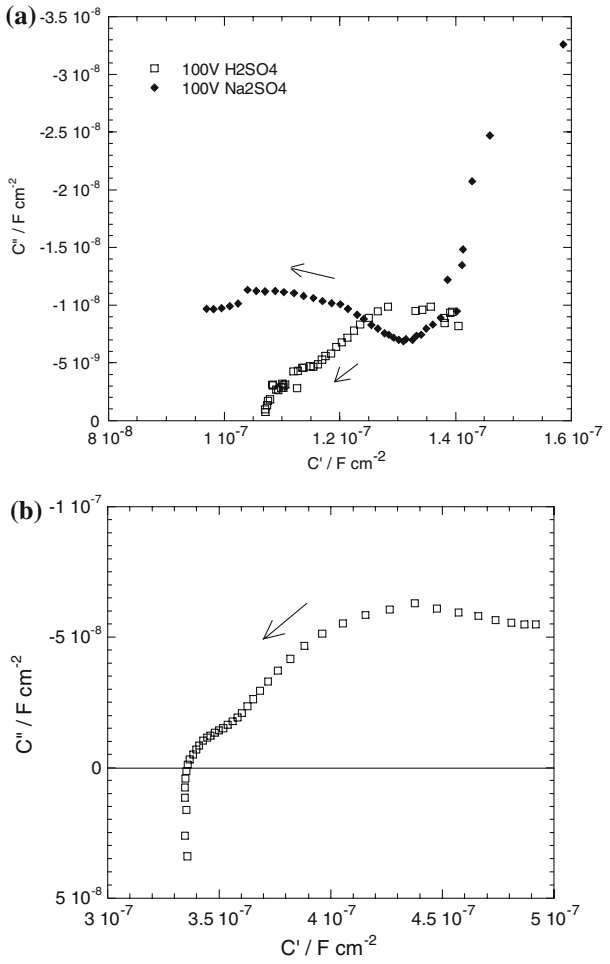

Fig. 7. Cole–Cole diagram of the impedance spectra between 10 Hz and 100 kHz after series resistance subtraction (the arrows show the direction of increasing frequencies) (a) films grown at 100 V in Na_2SO_4 and H_2SO_4; (b) film grown at 25 V in NaOH.

subsequent chemical etching. A marked increase in the impedance modulus is observed, which shows the formation of a surface layer during etching. This layer has been described in the literature as contaminated by F^- [20]. Using Equations (3) and (4) with $\varepsilon = 20$ its thickness is estimated as ranging between 5 and 7 nm. Accordingly, in the present study the thick films are not grown on bare metal, but at the interface between metal and a pre-existing thin zirconia film. Figure 1 shows that in spite of the presence of this pre-existing layer on the as-prepared electrode, a more or less intense oxygen evolution reaction occurs at the beginning of the potentiodynamic scan.

The same procedure can be used to estimate the electrode capacitance of the polished sample and gives circa. 7 μF cm^{-2}.

4.4. *Film growth rate*

We have shown in Section 4.2 that the oxide film thickness can be determined in the growth medium from the parameters of the high frequency CPE. However, in Equation (4) ε is an unknown parameter. Although it is generally assumed that the dielectric constant of zirconia is close to 20 [4, 20], values up to 38.3 can be found in the literature [21, 22]. This parameter is described as depending upon the electrolyte used since some anions can be inserted in thick zirconium oxide layers [4, 23, 24]. High calculated dielectric constants can be due to an overestimation of the film thickness measured from the charge exchanged (e.g. [19]), whereas side reactions can occur giving oxide film growth efficiencies lower than 1. The use of rather low frequency impedance measurements and the absence of dispersion correction by most authors can also lead to overestimation of this value.

Correlation between the EIS data and the film thickness was made by means of Equation (4). For a given solution and sweep rate, v_b, the dielectric constant ε was estimated by fitting C_f calculated from EIS data and several d assessed by SEM layer observation. In 0.5 M H_2SO_4 the best fit between SEM and the EIS data is found for ε equal to 20.8 (Figure 8a and Table 1), irrespective of v_b. The thickness measurements at different voltages and for the two different sweep rates are reported in Figure 8a. An important feature is that the slope, k, increases slightly with voltage. Another property of this medium is the decrease in the growth constant with sweep rate. Zirconia is reported as soluble in acidic medium [25] and the variation of k with E may be due to dissolution of the film at low voltage. The maximum layer thickness obtained here is 340 nm at 180 V and 100 mV s^{-1} and the layer is dense prior to breakdown.

The maximum anodisation voltage is not significantly improved in Na_2SO_4 (Figure 8b) with values ranging between 190 and 205 V (Figure 8b and Table 1). The best fit between SEM and EIS results is obtained with a dielectric constant equal to 18. The maximum film thickness at 340 nm is the same as that observed in H_2SO_4. The growth constant, k, is low at 1.7 nm V^{-1} but constant with applied voltage (Table 1).

In NaOH the best fit between EIS and SEM data was obtained for $\varepsilon = 19.5$ (Figure 8c and Table 1). Accordingly, no clear relationship is found between the dielectric constant of the films and the pH of the growth medium. In NaOH there is no influence of v_b on both ε and the growth rate. The film thickness varies linearly with applied voltage and the growth constant is 2.4 nm V^{-1} (Table 1). As breakdown occurs at 300 V, the maximum total film thickness reached in NaOH is circa 720 nm. The electric field in the film during growth is very high and constant, measured at 4.2×10^6 V cm^{-1} if we neglect the potential drop at the interfaces.

4.5. *Faradaic efficiency of film growth*

From the charge exchanged during the potentiodynamic scan (Figure 1) and the film thickness measured by EIS and SEM (Figure 8) it is possible to calculate the faradaic efficiency, noted ρ, of the electrochemical reaction (1) for film formation. The results obtained

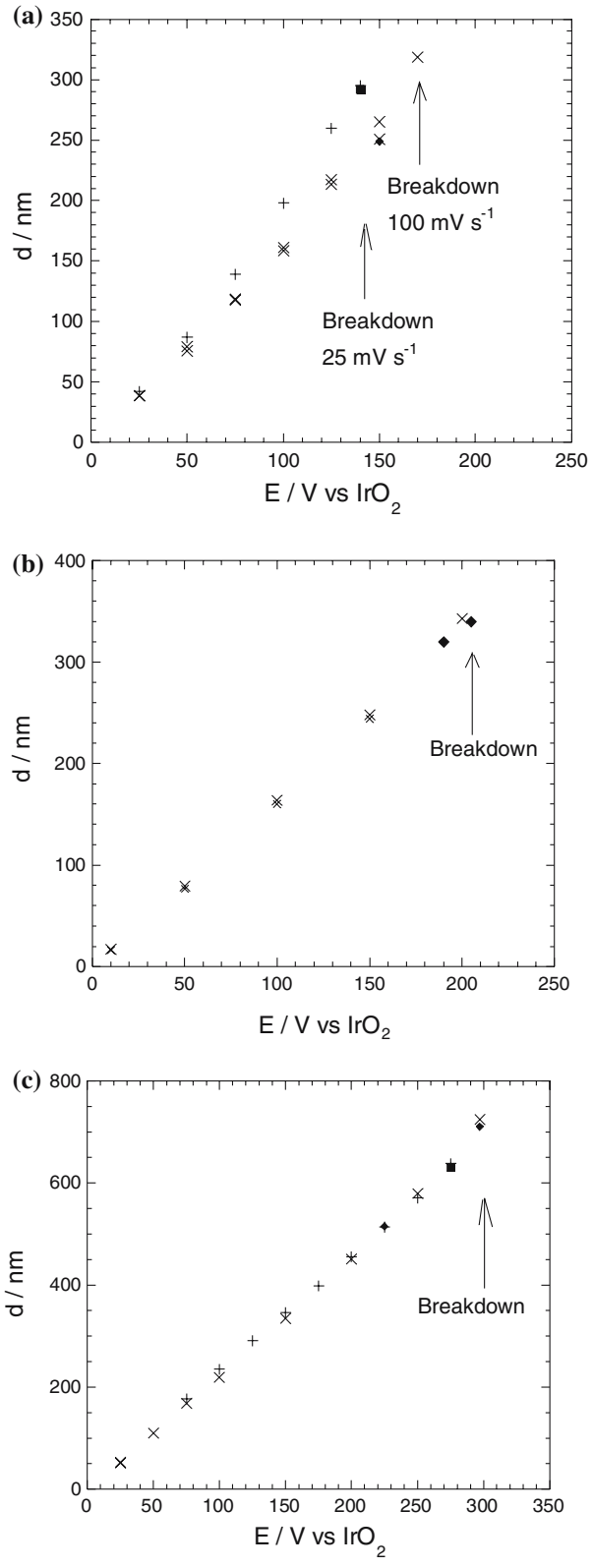

Fig. 8. Variation of film thickness with the applied voltage in various anodisation solution: (a) 0.5 M H_2SO_4, (b) 0.1 M Na_2SO_4 and (c) 0.1 M NaOH. EIS measurements (+) $v_b = 25$ mV s^{-1}, (X) $v_b = 100$ mV s^{-1} and SEM observation (◆) $v_b = 100$ mV s^{-1}, (■) $v_b = 25$ mV s^{-1}.

before breakdown in the different media are summarised in Table 2. The values are surprisingly low and the highest efficiency is obtained in H_2SO_4 even though

Table 1. Dielectric and growth constants of anodic zirconia in various media determined from the correlation between SEM observation and EIS measurements

Medium	pH	ε	v_b/mV s^{-1}	Growth constant /nm V^{-1}
0.5 M H_2SO_4	0.3	20.8	100	1.7/2.1
			25	2.1/2.3
0.1 M Na_2SO_4	9	18	100	1.7
0.1 M NaOH	13	19.5	100	2.4
			25	2.4

Table 2. Determination of dense film growth faradaic efficiencies, ρ in various media

Medium	pH	Potential /V	v_b /mV s^{-1}	Q^a_{exp} /C cm^{-2}	d^b_{exp} /μm	d^c_{th} /μm	ρ/%
0.5 M H_2SO_4	0.3	170	100	1.3	0.32	0.74	43
0.1 M Na_2SO_4	9	190	100	2.9	0.32	1.63	20
0.1 M NaOH	13	290	100	5.55	0.72	3.1	23

[a]Obtained by integration of Figure 1 curves.
[b]Measured on Figure 8.
[c]Theoretical thickness, calculated from Faraday's law, assuming a 4 electron reaction process and a film density of 5.68 g cm^{-3}. The molar mass of ZrO_2 is 123.2 g mol^{-1}.

ZrO_2 is reported as soluble in acidic media [25]. Accordingly side reactions occur during growth likely due to some electronic leakage. The main side reaction is likely oxygen evolution at the oxide/electrolyte interface.

4.6. *Meaning of the low frequency impedance in NaOH medium*

Compared to sulphate media, more complex impedance behaviour has been found in NaOH above 25 V. Two relaxations are recorded. The high frequency relaxation behaviour (above around 1 kHz) has been ascribed to anodic film growth (Section 4.2). The low frequency part little changes during the voltage scan. The more complex equivalent circuit can be explained by the formation of an anodic coating with two different electrical properties. An inner layer would be similar to that obtained in sulphate medium with a capacitive behaviour. The presence of the resistance R_2 may be due to higher electrical conductivity of the outer layer.

The presence of two layers is not observed by SEM. In the present state of the art it is difficult to speculate about the process which leads to the increase in film conductivity above a certain thickness limit. It may be induced by the formation of very fine channels filled by electrolyte. In this case R_2 would be the electrolyte resistance through the pores of the outer oxide film. The investigation of the anodic films by, for instance, high resolution TEM would give more detailed information on the structural features giving rise to a change in the electrical response. However, the bi-layered structure is

likely the result of a stress relaxation which could explain the higher breakdown voltage attained in NaOH compared to sulphate media in which the growth of a dense film seems to be limited at 300–340 nm, depending upon the sweep rate.

5. Conclusions

A procedure based on EIS measurements was described for zirconia film thickness monitoring during metallic zirconium anodisation. The films grown in the presence of sulphate anions are "dense" up to the breakdown potential, but this latter phenomenon arises at rather low voltage and the maximum film thickness obtained is measured at 340 nm. In contrast, in 0.1 M NaOH a structural transition is observed at 25 V ascribed to the formation of a bi-layered structure with an outer layer of a higher conductivity. The anodisation can be continued up to 300 V and the maximum total film thickness attained is 720 nm. Work is in progress to find new electrolytic media in which anodisation could be continued at much higher voltage, the micrometer range being a target for comparing these anodic films to those obtained by high pressure, high temperature corrosion before the kinetic transition [2].

Acknowledgements

The authors are grateful to X. Montero for anodisation experiments in Na_2SO_4 solutions. We thank Dr. D. Lincot (Laboratoire d'Électrochimie et Chimie Analytique, ENSCP), Dr. J Schefold and Dr. A. Ambard (EDF Research and development, Département Matériaux et Mécanique des Composant, Morêt sur Loing, France) for fruitful discussions of the results.

References

1. P. Meisterjahn, H.W. Hoppe and J.W. Schultze, vana. *J. Electroanal. Chem.* **217** (1987) 15.
2. J. Schefold, D. Lincot, A. Ambard and O. Kerrec, vana. *J. Electrochem. Soc.* **150** (2003) B451.
3. M. Cassir, F. Goubin, C. Bernay, P. Vernoux and D. Lincot, vana. *Appl. Surf. Sci.* **193** (2002) 120.
4. F. Di Quarto, S. Piazza and C. Sunseri, vana. *J. Electrochem. Soc.* **130** (1983) 1014.
5. N. Khalil, A. Bowen and J.S.L. Leach, vana. *Electrochim. Acta* **33** (1988) 1721.
6. E.M. Patrito, R.M. Torresi, E.P.M. Leiva and V.A. Macagno, vana. *J. Electrochem. Soc.* **137** (1990) 524.
7. L. Zhang, D.D. Macdonald, E. Sikora and J. Sikora, vana. *J. Electrochem. Soc.* **145** (1998) 898.
8. J.A. Bardwell and M.C.H. MacKubre, vana. *Electrochim. Acta* **36** (1991) 647.
9. J.S.L. Leach and B.R. Pearson, vana. *Electrochim. Acta* **29** (1984) 1263.
10. F. Di Quarto, S. Piazza and C. Sunseri, vana. *J. Electrochem. Soc.* **131** (1984) 2901.
11. J.S.L. Leach and B.R. Pearson, vana. *Corros. Sci.* **28** (1988) 43.
12. G.C. Wood and C. Pearson, vana. *Corros. Sci.* **7** (1967) 119.
13. C. Bataillon and S. Brunet, vana. *Electrochim. Acta* **39** (1994) 455.
14. J.J. Vermoyal, A. Frichet, L. Dessemond and A. Hammou, vana. *Electrochim. Acta* **45** (1999) 1039.
15. A.K. Jonscher, *Dielectric Relaxation in Solids* (Chelsea Dielectric Press, London, 1983).
16. A.K. Jonscher, vana. *J. Mater. Sci.* **16** (1981) 2037.
17. A.K. Jonsher, vana. *Nature* **253** (1975) 717.
18. G.J. Brug, A.L.G. Vanden Eeden, M. Sluyters-Rehabach and J.H. Sluyters, avna. *J. Electroanal. Chem.* **176** (1984) 275.
19. J.W. Schultze and K.J. Vetter, vana. *Ber. Bunsenges. Phys. Chem.* **75** (1971) 470.
20. E.M. Patrito and V.A. Macagno, vana. *J. Electrochem. Soc.* **140** (1993) 1576.
21. J.A. Bardwell and M.C.H. MacKubre, vana. *Electrochim. Acta* **36** (1991) 647.
22. J.L. Ord and D.J. Smet, vana. *J. Electrochem. Soc.* **142** (1995) 879.
23. M.A.A. Rahim and M.W. Khalil, vana. *J. Appl. Electrochem.* **26** (1996) 1037.
24. J.S.L. Leach and B.R. Pearson, vana. *Electrochim. Acta* **29** (1984) 1263.
25. M. Pourbaix, *Atlas d'équilibre électrochimiques à 25* °C (Gauthier-Villars, Paris, 1963), pp. 226.